MAGNETIC-FREE ELECTRICAL CIRCULATOR BASED ON ALN MEMS FILTERS AND CMOS RF SWITCHES

Changting Xu[1], Enes Calayir[1], and Gianluca Piazza[1]
[1]Electrical and Computer Engineering, Carnegie Mellon University, USA

ABSTRACT

This work reports the demonstration of a novel magnetic-free electrical circulator topology that facilitates the development of in-band full duplexers (IBFD) for simultaneous transmit and receive (STAR) RF applications. It uses CMOS-integrable components such as AlN MEMS filters (first-order in this work at 1.2 GHz) and CMOS RF switches, hence showing a compact approach that can be used in handheld devices. The linear time-invariant (LTI) AlN MEMS filter networks are parametrically modulated via a switching matrix to break its reciprocity. The modulation frequency and duty cycle were optimized so that the circulator can provide up to 15 dB of isolation over the filter bandwidth (2.2 MHz). The proposed prototype is a very compact solution for the implementation of magnetic-free circulators, which also intrinsically offers low noise and high linearity.

INTRODUCTION

The ever-increasing demand of data exchange has been driving the need for higher speed and larger capacity in wireless communications. This need requires rethinking the way RF front-ends are designed. Conventionally, RF front-ends rely on either time-division duplexing (TDD) or frequency-division duplexing (FDD) after the antenna (Ant) to isolate receiver (Rx) and transmitter (Tx) paths. This means that they transmit and receive either at different times, or over different frequency bands. However, considering the limitation in the available electromagnetic (EM) spectrum, these approaches are inefficient. An alternative approach is to replace the conventional duplexers with circulators, which allow simultaneous transmit and receive (STAR) at the same frequency and thus increase the efficient utilization of the EM spectrum [1, 2]. Circulators, allowing unidirectional (or non-reciprocal) signal power transmission, are usually implemented by passive nonreciprocal ferrite materials [3], which are bulky and cannot be integrated on chip, hence making STAR impractical in hand-held devices. Non-reciprocity can also be achieved by transistor-based networks [4, 5], but they exhibit poor linearity and noisy performance [6]. Recently, circulators based on angular momentum biasing [7] and staggered commutation have been investigated [8]. The former is limited by the low modulation ratio and nonlinearity of varactors, while the latter requires high *Q* off-chip inductors to reduce its waveguide length (~30cm).

To address the above issues, this work proposed a novel generalized circulator topology comprised of two identical linear-time-invariant (LTI) networks (blue and black colors in Fig. 1a) with 3-fold rotational symmetry parametrically modulated by normal/complementary pairs of switches with a rotational phase difference of 120° (see Figure 1b). In this work, the generalized LTI networks are formed by first-order AlN MEMS filters (*i.e.* two-port resonators) at 1.2 GHz [9] connected in a Δ-shaped configuration. Furthermore, this topology utilizes CMOS RF switches, and comes with four main advantage with respect to varactor-based networks: i) it is much easier to operate because it can be turned on and off by digital signals and eliminates complex off-chip biasing networks that are required by varactors; ii) the modulation ratio can be easily adjusted between 0 and 1 by tuning the duty cycle; iii) it provides effective modulation without adding significant losses when the modulation elements are added in series with the filter network (differently from varactors); iv) it prevents the noise coming from the modulation signals to be injected onto the carrier signal. By properly selecting the modulation frequency and duty cycle, more than 15-dB isolation between Rx and Tx was achieved over the filter bandwidth (2.2 MHz). Since the filter network and switches are all compatible with CMOS technologies, this work constitutes a very compact solution for the implementation of magnetic-free circulators.

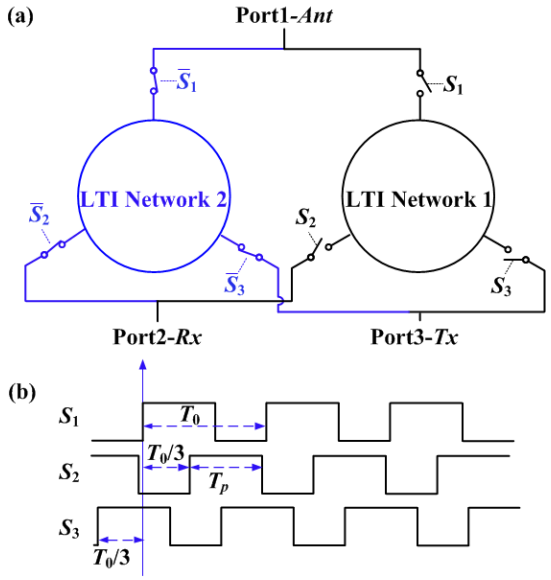

Figure 1: (a) Schematic representation of the proposed non-reciprocal network based on the parametric modulation of two identical LTI networks (1 and 2) with 3-fold rotational symmetry. (b) The 120° rotational phase relationships between modulation signals (square wave pulses). T_0 is the modulation period (1/frequency) and T_p is the pulse width. Duty cycle, α, is defined by the ratio of T_p to T_0.

DESIGN

Reciprocity is a fundamental property of LTI electrical networks. To break reciprocity, one common way is to introduce time-variant components. Figure 1a shows the schematic representation of the proposed circulator: two identical LTI networks with 3-fold rotational symmetry are parametrically modulated by a switch matrix. The modulation signals used to drive the switches of the black

branch are shown in Figure 1b, which are three digital pulse trains with the same period but a phase difference of 120° with respect to each other. The modulation signals of the blue branch complement that of the black one such that the RF input from the antenna is commutated between the two branches. The implementation of this topology is shown in Figure 2, where each LTI network is formed by three filters wire-bonded on a PCB and ADI single-pole-double-throw (SPDT) switches are used to implement those 3 normal/complementary pairs of switches. The filters are two-port AlN MEMS resonators (see Figure 3a) and are connected in a Δ-shaped network, as shown in Figure 3b. The non-identical responses and the apparent lack of 3-fold rotational symmetry are due to variations in wire bonding length and PCB traces.

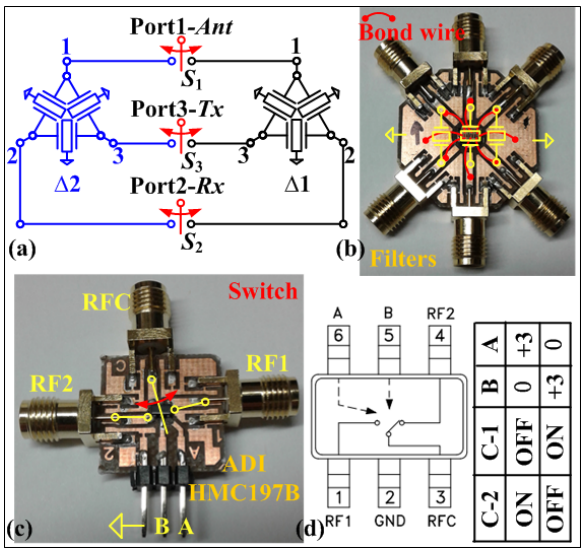

Figure 2: (a) The implementation of the circulator of Figure 1a. (b) PCB for wire-bonding three AlN MEMS filters. (c) PCB for a single CMOS RF switch. (d) Pin configuration of the CMOS RF switch and the corresponding truth table.

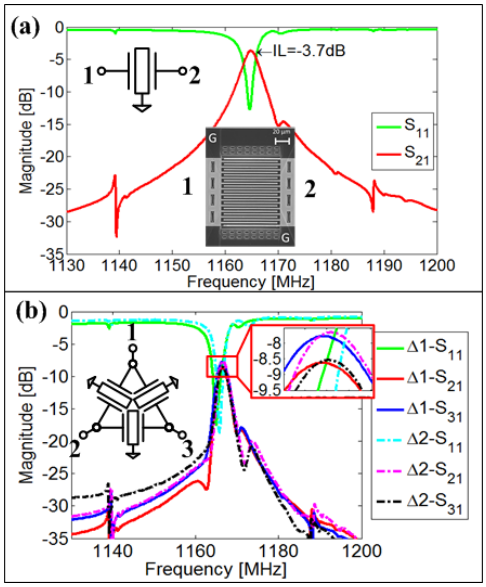

Figure 3: (a) The response of a first-order resonant filter wire-bonded on PCB. (b) The response of the two Δ networks (Δ1 and Δ2) used to implement the circulator.

Although the architecture may look similar to the angular-momentum biasing of a resonant ring in [11, 12], its behavior cannot be easily modeled by the temporal coupled-mode theory (CMT) presented in [13]. The switches impose much stronger modulation than varactors. The modulation effect can be characterized by the modulation ratio and the number of effective intermodulation products. The modulation ratio is defined as the ratio of first harmonic amplitude of the complex Fourier transform to the average amplitude. For a varactor that is modulated as

$$C(t) = C_0 + \delta C_0 \cos \omega_0 t, \tag{1}$$

where $C(t)$ is the real-time capacitance, C_0 the static capacitance, δ the modulation amplitude, and ω_0 the modulation frequency, the modulation ratio is $\delta/2$. The maximum value of δ is limited by the tuning ratio of varactors, η (which is defined as the ratio of the maximum capacitance to the minimum capacitance), which is given by

$$\delta \le \frac{\eta - 1}{\eta + 1} \tag{2}$$

Therefore, the modulation ratio of varactors is never greater than 0.5. Even worse, varactors experience a trade-off between quality factor and tuning ratio [14]. Therefore, the modulation ratio used in [13] is typically less than 0.05. Because of the small modulation ratio and sinusoidal modulation pattern, it is enough to consider only three intermodulation frequencies, ω_{RF}, $\omega_{RF} \pm \omega_0$, where ω_{RF} is the RF carrier frequency. The reduced number of frequencies dramatically simplifies the analysis via CMT. In contrast, the modulation ratio of a switch turned on and off with a duty cycle of α is $|\mathrm{sinc}(\alpha\pi)| \in [0,1]$. For example, $|\mathrm{sinc}(\alpha\pi)| = 0.64$ when $\alpha = 0.5$. Due to the square modulation pattern, it is necessary to take more than 25 intermodulation products into account to accurately predict the circulator response.

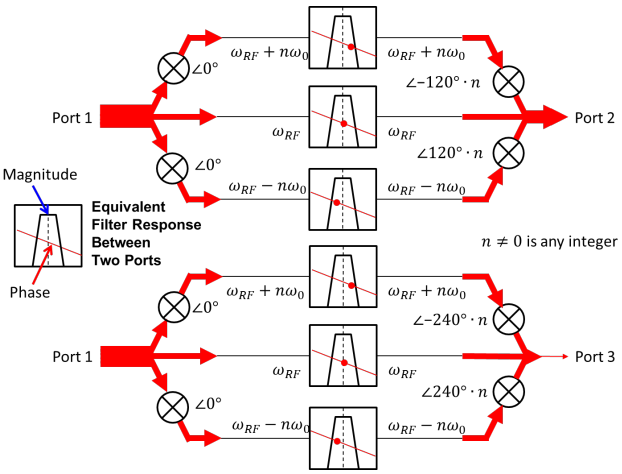

Figure 4: Schematic representation of different phase shifts of power transfer in different "paths".

Furthermore, the resonant rings (resonator networks) in this work support more than 3 modes (6 resonators connected in the network), which renders CMT too complex to analyze the proposed circulators. Lastly, the way in which the switches interact with the resonant network is different from what happens with varactors,

which actually alter the center frequency of operation of the network, an important factor that needs to be accounted for when designing the circulator passband [12].

Herein a qualitative and straightforward explanation of the working principle is provided through an analysis in the frequency domain (see Figure 4). The switching modulation converts the RF carrier frequency, ω_{RF}, to many intermodulation frequencies, $\omega_{RF} + n\omega_0$, where n is an integer, thus generates different "paths" for power transfer from one port to the other two ports. Part of the RF power from antenna (Port 1) can be transferred to the receiver/transmitter (Port2/3) directly without any frequency conversion. The rest of the power is first up/down converted to the intermodulation frequencies at Switch S_1, and then down/up converted to the RF carrier frequency at S_2 and S_3. Because of different phase shifts introduced in different paths (due to modulation phase and filter spectral phase), the signals can be made to add up constructively when flowing in a particular direction (e.g. from the antenna to the receiver), and destructively when in another (e.g. from the transmitter to the receiver). The effectiveness of the non-reciprocity is controlled by the frequency and duty cycle of the modulation.

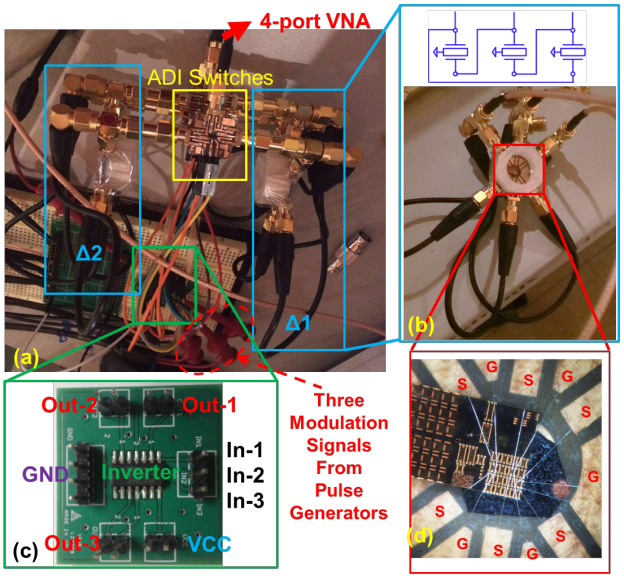

Figure 5: (a) The experimental setup of the proposed circulator in Figure 2a. (b) The connection method of the Δ-networks. (c) PCB design for the hex inverter. Each Out-k (k=1-3) is a pair of pins, carrying two signals, one of which is the same as In-k (k=1-3), the other is its complementary. (d) The optical image of wire-bonded resonators on PCB. The chip is formed by a 4-by-4 array of identical resonators. Three of these 16 resonators are chosen for this experiment.

EXPERIMENTAL RESULTS

We implemented the circulators with discrete AlN MEMS filters and CMOS RF switches, which were separately wirebonded onto two PCBs (see Figure 5b and d). These PCBs were then connected through SMA cables/adaptors (see Figure 5a). As for the modulation signals, three pulse trains are generated by two synchronized 2-output pulse generators, Agilent 81110A. These pulse trains are then fed to a hex inverter, 74HCT04, to generate 3 complementary pairs of square waves (see Figure 5c). The phase differences between these signals were monitored by a 4-channel oscilloscope, Agilent DSO6014, and are automatically adjusted to be 120° by a MATLAB program. The S-parameters are measured using an Agilent 4-port network analyzer, N5230A, after performing SOLT calibration.

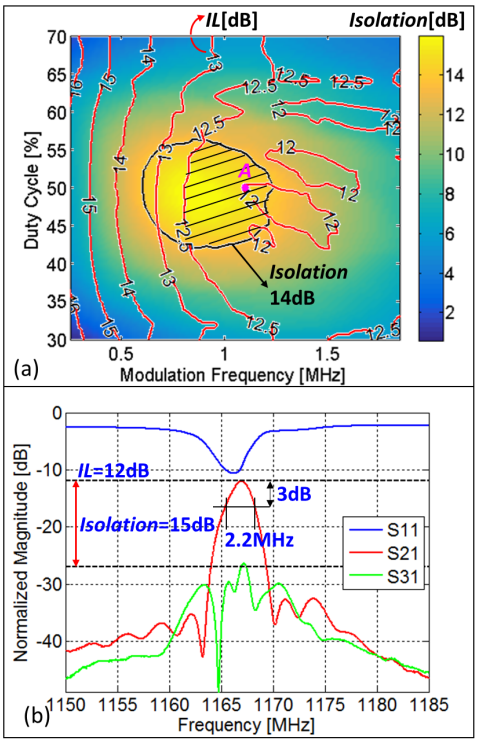

Figure 6: (a) The contour plot of IL (red lines) and isolation (background color) with respect to the modulation frequency and duty cycle for a first-order filter based circulator. (b) The response of the circulator when modulated at 1.1MHz with 50% duty cycle (Point A in Figure 6a).

The modulation frequency and duty cycle were swept to investigate their effect on insertion loss (*IL*) and isolation of the circulator, as shown in Figure 6a. It can be observed that there is a sort of trade-off between modulation frequency and duty cycle. At this point in time, the reason behind this trade-off is not fully understood. Nonetheless, this experimental characterization facilitates the selection of the optimal modulation frequency and duty cycle so as to simultaneously attain the lowest *IL* and largest isolation. The S-parameters of the circulator using the modulation parameters at Point *A* are shown in Figure 6b. Interestingly, more than 15 dB of isolation can be attained over the entire bandwidth of the filter(2.2 MHz), in contrast to the narrow-band rejection demonstrated in [7] and [8]. The *IL* of the demonstrated circulator is 12 dB. We have analyzed the main sources of loss in this configuration and listed them in Table 1. The mechanisms that account for ~6 dB loss still remain unclear. The plausible causes are asymmetries in the filters, the modulation process itself, delays in the inverter controlling the switching process, and glitches in the inverter outputs (observed especially beyond 1 MHz). Among the loss factors, PCB loss and the deviations in the implementation

from rotational symmetry are expected to be significantly reduced by monolithic integration of the switches with the AlN devices.

CONCLUSION

We demonstrated the AlN MEMS filter based circulators at 1.2 GHz, which achieve 15 dB isolation over the entire filter bandwidth (2.2 MHz) with a modulation at 1.1 MHz. The proposed circulators are easily integrated into CMOS processes, and are expected to be highly linear and exhibit low noise. The insertion loss can be improved by monolithic integration and by resorting to a differential circulator topology [15]. Future work will focus on optimizing the filter impedance to offer better match to 50 Ω and the development of an analytical model that correctly depicts the losses due to the modulation process.

Table 1: Estimated contributions to the IL of the circulator. Units are in dB.

Factor	Contribution
Filter Loss + PCB Loss①	~3.7
Switch Loss	~1.1
Mismatch②	~0.9
Leakage to Tx③	~0.3
Unknown Loss④	~6.0
Total	**12**

①PCB Loss is measured to be around 1 dB in this work.
②calculated as $20\cdot\log_{10}(1-|S_{11}|^2)$. In this work, $S_{11} = 0.32$ (–10 dB).
③calculated as $20\cdot\log_{10}(1-|Iso|^2)$, where *Iso* means the isolation between Rx and Tx (the ratio of S_{31} to S_{21}). In this work, *Iso* = 0.18 (–15 dB).
④calculated by subtracting the first four types of loss from the total loss.

REFERENCES

[1] D. Bharadia, E. McMilin, and S. Katti, "Full duplex radios," *ACM SIGCOMM Computer Communication Review,* vol. 43, pp. 375-386, 2013.

[2] A. Sabharwal, P. Schniter, D. Guo, D. W. Bliss, S. Rangarajan, and R. Wichman, "In-band full-duplex wireless: Challenges and opportunities," *IEEE Journal on Selected Areas in Communications,* vol. 32, pp. 1637-1652, 2014.

[3] D. M. Pozar, *Microwave engineering*, John Wiley & Sons, 2009.

[4] S. Tanaka, N. Shimomura, and K. Ohtake, "Active circulators—The realization of circulators using transistors," *Proceedings of the IEEE,* vol. 53, pp. 260-267, 1965.

[5] G. Liming, C. Wenquan, F.-H. Huang, and H.-C. Chiu, "A high power active circulator using GaN MMIC power amplifiers," *Journal of Semiconductors,* vol. 35, p. 115003, 2014.

[6] G. Carchon and B. Nanwelaers, "Power and noise limitations of active circulators," *IEEE Transactions on Microwave Theory and Techniques,* vol. 48, pp. 316-319, 2000.

[7] N. A. Estep, D. L. Sounas, J. Soric, and A. Alù, "Magnetic-free non-reciprocity and isolation based on parametrically modulated coupled-resonator loops," *Nature Physics,* vol. 10, pp. 923-927, 2014.

[8] N. Reiskarimian and H. Krishnaswamy, "Magnetic-free non-reciprocity based on staggered commutation," *Nature communications,* vol. 7, 2016.

[9] G. Piazza, P. J. Stephanou, and A. P. Pisano, "One and two port piezoelectric higher order contour-mode MEMS resonators for mechanical signal processing," *Solid-State Electronics,* vol. 51, pp. 1596-1608, 2007.

[10] *HMC197B(E) - Analog Devices*. Available: http://www.analog.com/media/en/technical-documentation/data-sheets/hmc197b.pdf

[11] N. Estep, D. Sounas, and A. Alù, "On-chip non-reciprocal components based on angular-momentum biasing," in *Microwave Symposium (IMS), 2015 IEEE MTT-S International*, 2015, pp. 1-4.

[12] M. M. Torunbalci, T. J. Odelberg, S. Sridaran, R. C. Ruby, and S. A. Bhave, "An FBAR Circulator," *arXiv preprint arXiv:1710.05003,* 2017.

[13] N. A. Estep, D. L. Sounas, and A. Alù, "Magnetless microwave circulators based on spatiotemporally modulated rings of coupled resonators," *IEEE Transactions on Microwave Theory and Techniques,* vol. 64, pp. 502-518, 2016.

[14] M. Tiggelman, K. Reimann, F. Van Rijs, J. Schmitz, and R. J. E. Hueting, "On the trade-off between quality factor and tuning ratio in tunable high-frequency capacitors," *IEEE transactions on Electron Devices,* vol. 56, pp. 2128-2136, 2009.

[15] A. Kord, D. L. Sounas, and A. Alù, "Pseudo-Linear-Time-Invariant Magnet-less Circulators Based on Differential Spatio-Temporal Modulation of Resonant Junctions," *arXiv preprint arXiv:1709.08133,* 2017.

CONTACT

*C. Xu, changtix@andrew.cmu.edu
*G. Piazza, piazza@ece.cmu.edu